Glass–fibre–reinforced Polymer

Subjects: Polymer Science | Engineering, Civil

Contributor: Yiqing Dai , Xuewei Dai , Yu Bai , Xuhui He

Wind barrier structures are usually installed on railway bridges to reduce wind effects on travelling trains for safety considerations. This however adversely transfers wind loads and causes associated aerodynamic effects to the bridge. An innovative concept of wind barriers using glass fibre reinforced polymer (GFRP) composites is proposed in this work with experimental investigations and numerical modelling. This work provides a solution to mitigate the wind and associated aerodynamic loads. With an appropriate design of bending stiffness, the proposed barriers may deform adaptively in strong wind scenarios and let the wind to pass through their deformed shape and therefore transfer less load to the bridge. Wind-tunnel experiments and numerical studies are conducted on the aerodynamic responses of the train-barrier-bridge system under crosswind with various speeds. The influences of barrier height, air-flow speed and location of the train on the aerodynamic responses of the system were clarified. Both reduced-scale and full-scale finite element models were established for the train-barrier-bridge system and the results were validated with the experimental results to further support the research findings.

Fibre reinforced polymer | Wind barrier | Railway bridge | Aerodynamic coefficient | Wind-tunnel experiment | Aerodynamics

1. Introduction

Strong crosswinds may cause safety problems, such as shaking, derailment and overturning of travelling trains [1][2][3]. Apart from the limitation on the operating speed and the cancellation of train trips in strong-wind scenarios, wind barriers have also been used to mitigate the negative effects of crosswind on trains [3][4], and are considered an effective and economical way [5][6] to improve the safety of travelling trains. However, for the bridges, this approach may in return cause additional wind loads associated with the aerodynamic effects acting on the wind barriers, which are transferred to the bridge. In order to ensure the safety of both travelling trains and the bridge, it may be required for the wind barrier to allow more or less wind to pass depending on the wind pressure level such that the wind load transferred to the structure can be reduced.

Wind tunnel tests [6][7][8][9] and numerical modelling [10][11][12][13] have been conducted to investigate the associated parameters to understand the aerodynamic performance of wind barriers and trains. For example, the effects of airflow speed, train speed and wind directions on the aerodynamic performance of a train with a rigid wind barrier were investigated through wind tunnel tests. It was concluded that a scenario with a static train is more critical than those with moving trains in terms of the mechanical loads on the train caused by the crosswind; meanwhile, the effect of airflow speeds on the aerodynamic coefficients of the train is insignificant [6]. In order to investigate the

effect of the relative angle between the crosswind and the train (i.e., the yaw angle) on the mechanical responses of the train–barrier–bridge system, a numerical model of a railway system supported by a steel truss bridge was established using a computational fluid dynamics (CFD) method, where the simulation results were compared with those from wind tunnel experiments. It was suggested that airflow with a yaw angle of 90° (i.e., perpendicular to the travelling direction of the train) would lead to the maximum side force and overturning moment on the train [13].

Therefore, the design of wind barriers (e.g., porosity and height) can introduce different effects on the aerodynamic performance of trains and bridges. In strong wind conditions, where train trips may be cancelled, or even during the time there are no trains travelling on the bridge, such shielding effects become unfavourable since adverse wind loads and the associated aerodynamic effects would be acting on the bridge. Several railways are supported on bridges [8]; therefore, the safety consideration for both travelling trains and supporting bridges with wind barriers needs to be addressed. Recently, louver-type wind barriers with adjustable blades were introduced [10][14], where the porosity of the wind barriers can be adjusted by changing the incline angle of the blades. Obviously, such louver-type wind barriers require adjustment of the blades, where this would become time-consuming and hard to operate if completed manually, or would have a high cost and may not be reliable in harsh weather conditions (such as a strong wind) if completed automatically.

2. Material Properties of GFRP

GFRP materials have been used in bridge superstructures [15] and building structures [16][17][18] for their superior resistance to corrosion, high strength-to-weight ratio and competitive cost [19]. In this study, the wind barriers were made of GFRP plates with a thickness of 0.6 mm, which was chosen by considering the reduced scale and the bending stiffness requirements. The aerodynamic performance of the adaptive wind barrier is closely related to the elastic modulus of the plates, thus tensile tests on the GFRP plates were conducted.

The GFRP plate was prepared through a wet layup approach using epoxy resin and two layers of woven GFRP fabrics, resulting in a total thickness of 0.6 mm. Five sample specimens with dimensions of 250 × 25 mm^2 were cut from the same GFRP plate that was used for the wind barrier in the wind tunnel tests. Aluminium alloy plates with a length of 50 mm each were adhesively bonded to both ends of each GFRP specimen to protect the clamping area at both ends. As shown in Figure 1, two perpendicular strain gauges were installed at the centre of each GFRP specimen to obtain the strains in the longitudinal and transverse directions under loading. Tensile tests were conducted according to ASTM D3039 [20] for the five specimens. The load was applied using an MTS machine (MTS, Eden Prairie, MN, USA) at a loading rate of 2 mm/min until the failure of the specimens. The tensile loads and strain results were continuously recorded at 2 Hz during the loading process.

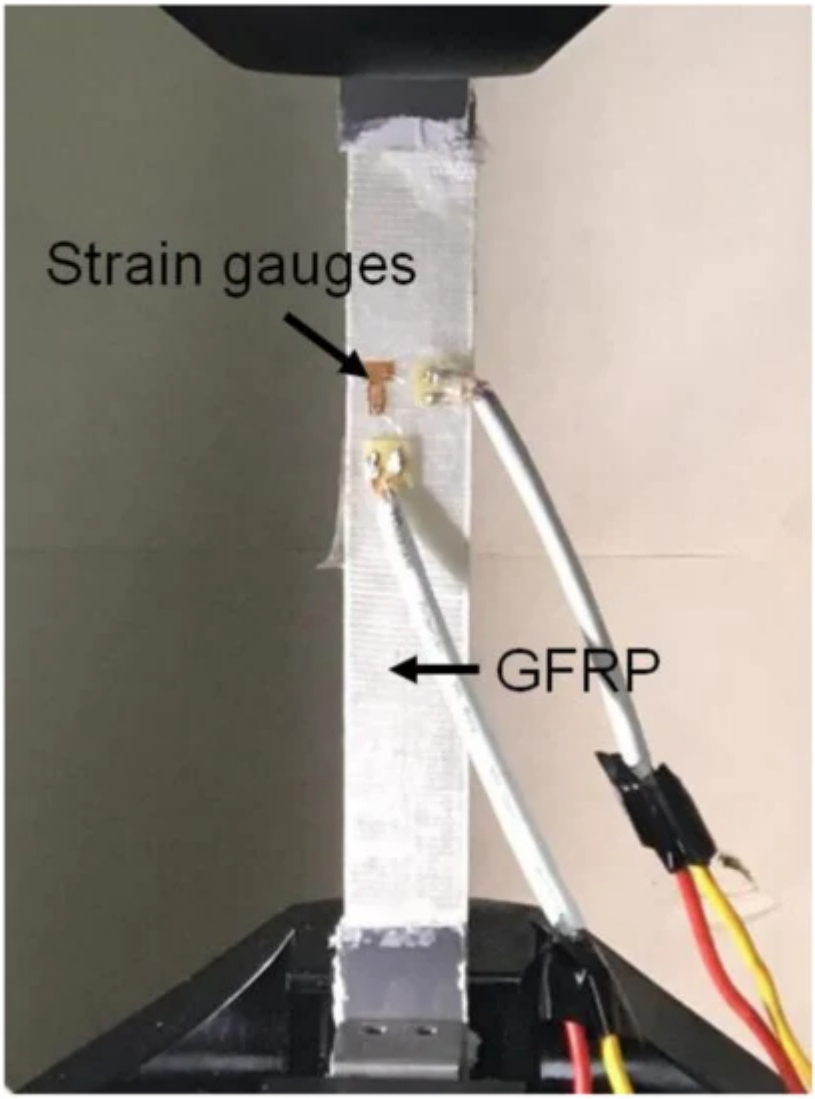

Figure 1. Tensile tests for the glass-fibre-reinforced polymer (GFRP) composite materials.

The ultimate stress of the GFRP specimens was obtained from their ultimate loads and nominal cross-sectional areas (i.e., 25 × 0.6 mm^2). The Poisson's ratio was obtained based on the strain gauge readout in the longitudinal and transverse directions, which was determined to be 0.183 on average. The ultimate stress was determined to be 216.6 MPa on average and the average elastic modulus was obtained as 8.6 GPa based on the linear elastic responses.

3. Conclusions

An innovative concept for a wind barrier was proposed to reduce the wind load transferred from the barrier to the bridge through the adaptive deformation of the barrier in crosswind scenarios. The barriers were made of GFRP composites with a relatively low bending stiffness, therefore allowing them to deform by bending more prominently in comparison to traditional wind barriers made from steel and reinforced concrete. Reduced-scale wind tunnel experiments were conducted to investigate the effects of the barriers on the aerodynamic performance of the train and bridge, including their side-force and overturning-moment coefficients. A reduced-scale FE model was

developed and its results were validated by comparing them with the experimental results. The validated modelling approach was then used to develop a full-scale train–barrier–bridge system to understand the mechanical and aerodynamic characteristics in practice. The following conclusions may be drawn from this work:

- The proposed wind barriers made from GFRP composites showed adaptive bending deformation when subjected to crosswind and more significant lateral deformation was seen with higher airflow speeds. Based on the results from the wind tunnel experiments, it can be seen that when the train was on the windward side on the bridge, both the train and the bridge were associated with a higher side-force and overturning-moment coefficients in comparison to the scenarios with the train in the leeward side or absent. For example, with a constant airflow speed of 10 m/s and a barrier height of 10 cm, the overturning-moment coefficient for the bridge (C_{BM}) was 0.162 when the train was on the windward side, while it became less than 0.148 for the other two scenarios.

- The wind tunnel experiments further showed that a wind barrier taller than 10 cm reduced the overturning-moment coefficient (C_{TM}) of the train from 0.41 (without the wind barrier) to be less than 0.08, and reduced the side-force coefficient (C_{TY}) of the train from 0.57 (without the wind barrier) to be less than 0.19. Therefore, the transfer of the wind load to the train could be effectively mitigated in this way. The values of C_{TM} and C_{TY} were not noticeably decreased when the barrier height was further increased from 10 cm to 13.5 cm. This suggests there may be an optimal height for the proposed wind barrier in terms of the aerodynamic performance of the train. Furthermore, when different airflow speed levels from 5 to 20 m/s were applied, the variations of C_{TM} and C_{TY} were insignificant, for example, within 10.5% for the former and 9.4% for the latter when the barrier height was 8 cm.

- The wind tunnel experiments also indicated that for an airflow speed over 10 m/s, the proposed wind barrier increased the overturning-moment coefficient (C_{BM}) of the bridge from 0.02 (without the wind barrier) to 0.15 (8 cm wind barrier) and increased the side-force coefficient (C_{BY}) of the bridge from 0.72 (no wind barrier) to 0.97 (8 cm wind barrier). Again, the effects of a change in the airflow speeds on C_{BY} was minor, while C_{BM} significantly decreased when the airflow speed rose from 10 to 20 m/s for all barrier heights applied. Such a decrease was more obvious for a taller barrier, for example, 9.4% for the 8 cm barrier and 25.2% for the 13.5 cm barrier. This was in association with the increases of deformation of the barriers with their heights and airflow speeds; therefore, the barrier with a larger deformation showed less resistance to wind and then transferred lower loads to the bridge.

- The results from the reduced-scale FE modelling were consistent with those from the wind tunnel experiments. The validated FE approach was used to develop the full-scale train–barrier–bridge system. The full-scale modelling results indicated that the change in C_{BY} with airflow ranging from 5 to 20 m/s was not obvious, with a variation of only 4%. However, the decrease in the overturning-moment coefficient of the bridge, C_{BM}, with the increase in the airflow speed was more prominent than the results from the wind tunnel experimental results. This suggests that the mitigation in the transfer of the wind load to the bridge by the proposed adaptive wind barrier was effective at the full scale in practice.

References

1. Argentini, T.; Ozkan, E.; Rocchi, D.; Rosa, L. Cross-wind effects on a vehicle crossing the wake of a bridge pylon. J. Wind Eng. Ind. Aerodyn. 2011, 99, 734–740.
2. Chen, S.; Cai, C.S. Accident assessment of vehicles on long-span bridges in windy environments. J. Wind Eng. Ind. Aerodyn. 2004, 92, 991–1024.
3. Xu, Y.L.; Zhang, N.; Xia, H. Vibration of coupled train and cable-stayed bridge systems in cross winds. Eng. Struct. 2004, 26, 1389–1406.
4. Olmos, J.M.; Astiz, M.A. Improvement of the lateral dynamic response of a high pier viaduct under turbulent wind during the high-speed train travel. Eng. Struct. 2018, 165, 368–385.
5. Kwon, S.; Kim, D.H.; Lee, S.H.; Song, H. Design criteria of wind barriers for traffic. Part 1: Wind barrier performance. Wind Struct. 2011, 14, 55–70.
6. Xiang, H.; Li, Y.; Chen, S.; Hou, G. Wind loads of moving vehicle on bridge with solid wind barrier. Eng. Struct. 2018, 156, 188–196.
7. Avila-Sanchez, S.; Lopez-Garcia, O.; Cuerva, A.; Meseguer, J. Characterisation of cross-flow above a railway bridge equipped with solid windbreaks. Eng. Struct. 2016, 126, 133–146.
8. He, X.; Zou, Y.; Wang, H.F.; Zou, Y.F.; Han, Y.; Shi, K. Aerodynamic characteristics of a trailing rail vehicles on viaduct based on still wind tunnel experiments. J. Wind Eng. Ind. Aerodyn. 2014, 135, 22–33.
9. Niu, J.; Zhou, D.; Liang, X.; Zhou, D. Experimental research on the aerodynamic characteristics of a high-speed train under different turbulence conditions. Exp. Therm. Fluid Sci. 2017, 80, 117–125.
10. He, X.; Shi, K.; Wu, T.; Zhou, Y.; Wang, H.; Qin, H. Aerodynamic performance of a novel wind barrier for train-bridge system. Wind Struct. 2016, 23, 171–189.
11. Liu, T.; Chen, Z.; Zhou, X.; Zhang, J. A CFD analysis of the aerodynamics of a high-speed train passing through a windbreak transition under crosswind. Eng. Appl. Comput. Fluid Mech. 2018, 12, 137–151.
12. Montenegro, P.A.; Calcada, R.; Carvalho, H.; Bolkovoy, A.; Chebykin, I. Stability of a train running over the Volga river high-speed railway bridge during crosswinds. Struct. Infrastruct. Eng. 2020, 16, 1121–1137.
13. Wang, M.; Li, X.; Xiao, J.; Zou, Q.-Y.; Sha, H.-Q. An experimental analysis of the aerodynamic characteristics of a high-speed train on a bridge under crosswinds. J. Wind Eng. Ind. Aerodyn. 2018, 177, 92–100.

14. He, X.; Fang, D.; Li, H.; Shi, K. Parameter optimization for improved aerodynamic performance of louver-type wind barrier for train-bridge system. J. Cent. South Univ. 2019, 26, 229–240.
15. Keller, T.; Schollmayer, M. Plate bending behavior of a pultruded GFRP bridge deck system. Compos. Struct. 2004, 64, 285–295.
16. Satasivam, S.; Bai, Y.; Yang, Y.; Zhu, L.; Zhao, X.L. Mechanical performance of two-way modular FRP sandwich slabs. Compos. Struct. 2018, 184, 904–916.
17. Gu, X.; Dai, Y.; Jiang, J. Flexural behavior investigation of steel-GFRP hybrid-reinforced concrete beams based on experimental and numerical methods. Eng. Struct. 2020, 206, 110117.
18. Dai, Y.; Bai, Y.; Keller, T. Stress mitigation for adhesively bonded photovoltaics with fibre reinforced polymer composites in load carrying applications. Compos. Part B-Eng. 2019, 177, 107420.
19. Bank, L. Composites for Construction Structural Design with FRP Materials; John Wiley & Sons: Hoboken, NJ, USA, 2006.
20. ASTM Committee D-30 on Composite Materials. Standard Test Method for Tensile Properties of Polymer Matrix Composite Materials; ASTM D3039/D3039M-17; ASTM International: West Conshohocken, PA, USA, 2017.